Wear experiments on PLA-Cu composite filament printed in different FDM conditions

M.Venkata Pavan[a], K. Balamurgan[a], P. Balamurgan[b]

[a]Department of Mechanical Engineering, VFSTR (Deemed to be University) Guntur - 522213, AP, India.
[b]Department of Mechanical Engineering, Kalasalingam Academy of Research and Education, Tamil Nadu, India.

Article History: Received: 10 January 2021; Revised: 12 February 2021; Accepted: 27 March 2021; Published online: 20 April 2021

Abstract: The fabricated 3D composite filaments are processed and evaluated for wear property using the pin on disc technique in a Fused Deposition Model (FDM). When measurements are taken under various machining conditions such as load, track diameter, and speed, Grey Relational Analysis (GRA) is used to optimize friction strength and wear rate. Some relevant similarities of those other metrics are found and documented using Analysis of Variance (ANOVA). It is notable that the applied test load appears to have a greater contribution of about 76 percent and appears to have a high effect on the sample's end quality. To check the findings, a validation experiment is also carried out.

Keywords*:* Composite 3D filament; Pin-on Disc; Friction; GRA

1. Introduction

The relevance includes its FDM became outlined reported by Fang et al., (Feng, 2017), while the FDM strategies have shown to be a particularly appropriate system with assembling sophisticated systems while external development throughout many industrial applications. According to Tuan et al., (Tuan, 2018),various fields of technologists identified some benefits of FDM likely to include design freedom, process engineering, reduced waste, and even the publishing of every other structural system.

For reference, (Gnanasekaran, 2017) prepared CNT and graphene-based conductive polymer nanocomposites for the electrical application using FDM, etc., the likely number of research works are being carried out to meet the engineering trends. The sample is utilizing multi-dimensional 3D PLA/graphene composite filament utilizing FDM has shown improved machining properties by (Prashantha, 2017). Ceramic materials used by (Najera, 2018) as reinforcements in the PLA matrix and printed using FDM has shown as phase separation between the elements and with a porous structure which could be used for bone replacement. Reported the orthotropic behaviors can indeed be detected with FDM where the observations are contradictory (Miguel, 2018).

According to metal powders with PLA structure have received popularity due to the possibility of almost any reflex includes complex shapes (Sheikh, 2010). To transform metal into yet another oxidized copper element, constructed 3D printed samples, including copper as reinforcement in the PLA and conducted sintering with insulation, and underwent polymerization towards making a 3D semiconductor that was sensitive to light, pressure, and temperature (Ahamad, 2017). Reported from the tests observed that a +45o/-45o raster angle offer suitable to have the highest mechanical stability and Young's modulus (Zhaobing, 2019; Evgeni, 2019). Through an analytical model with 3D printed samples, Found that perhaps the precipitation procedure alone does not evaluate the properties include its mechanical behavior besides subsequent processing likely compression will signify the mechanical property (Lebedev, 2019).

To calculate the effect of FDM specification on either the material characteristics, used the Taguchi orthogonal array (Uzair, 2019). According to the GRA approach was one of the best techniques used for the conversion of multiple objectives into a single. GRA was used to overcome various specific questions, unlike most of the Taguchi approach has a complicated entity, relational conflicts accurately estimated through using GRA. Again for machined surface review of Al7075 alloy, Babu et al., implemented the Taguchi optimized claimed along streamline approach changes the surface quality as well as tool life (Babu, 2019). Applied the Taguchi based GRA technique to find the optimum condition while turning Rock dust reinforced Aluminum Metal Matric Composite in different cutting conditions. (Prakash, 2020; Venkata Pavan, 2020; Balamurugan; 2018)

2. Materials and Methods

2.1 Preparation of composites.

A customized experimental setup was created in order to fabricate a PLA-copper filament, as shown in Figure 1. PLA and copper micro-powder with sizes ranging from 30 to 50 micro meter were obtained from the Coimbatore Material Mart in India. The PLA workpiece was machined into small particles, and 12 percent copper powder was added before the mixture was ball milled for 24 hours. Hopper is equipped with a heating element and is set to 195 degrees Celsius. A screw conveyor is used to create a 0.6mm diameter filament. The extruded filament was cold and water-based, and it was rolled in a stack. The filament has been produced and is ready to

print. According to Venkata Pavan and Balamurugan, using 12 percent copper particles as filler elements improves mechanical properties.

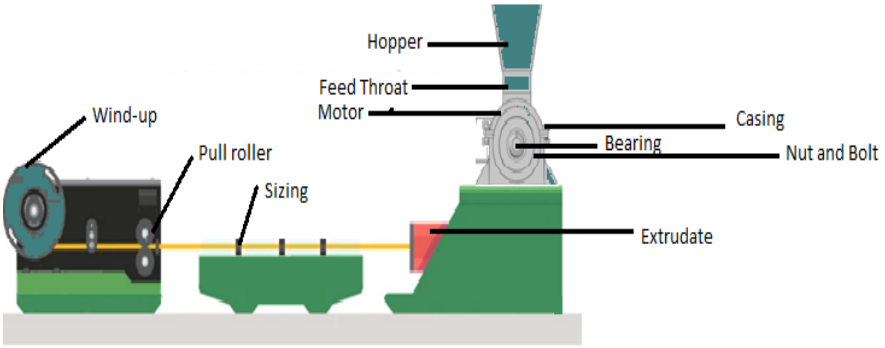

3D Composite Extruder

Figure 1. Experimental Setup

2.2 Experimental procedure.

The wear rate test was carried out on Ducom pin on disc equipment, model TR20LE-M5. Table 1 shows the FDM printing condition that was set. The sample surface was machined so that it was fully in contact with the wear disk, and the sample was fixed so that it was perfectly perpendicular to the disc. EN 31 steel was used to make the disc.

Table 1. Wear parameters and FDM machining condition

S.No	Factors	Levels			Units	Symbols
		1	2	3		
1	Load	21	31	41	N	A
2	Track Diameter	30	40	50	mm	B
3	Speed	310	410	510	rpm	C

The aim is to optimize the selected elements by comparing them at three different levels to each other in order to produce better output response is shown in Figure 2. The Degree Of Freedom (DOF) of the three variables was calculated according to the total number of levels (n) for each parameter minus one to determine the required orthogonal matrix (n-1). As a result, the orthogonal network L27 was computed for an optimist.

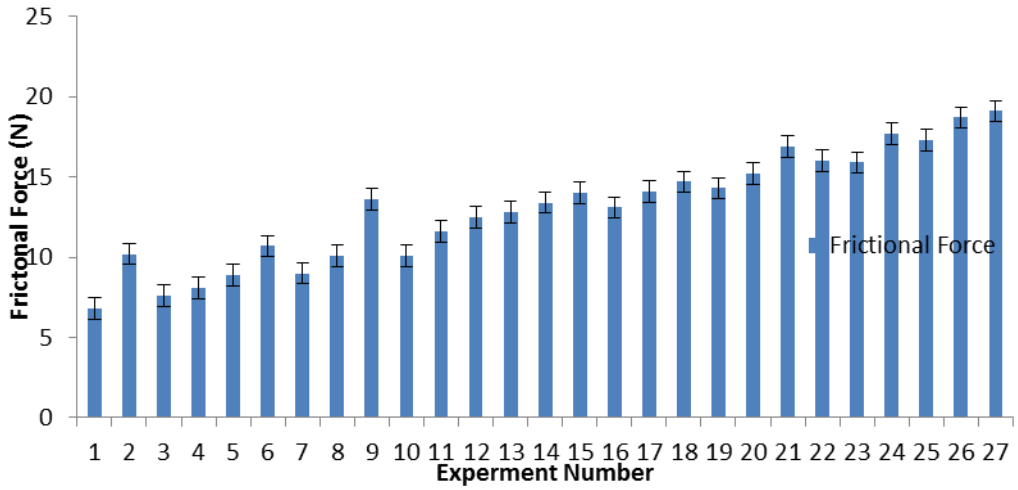

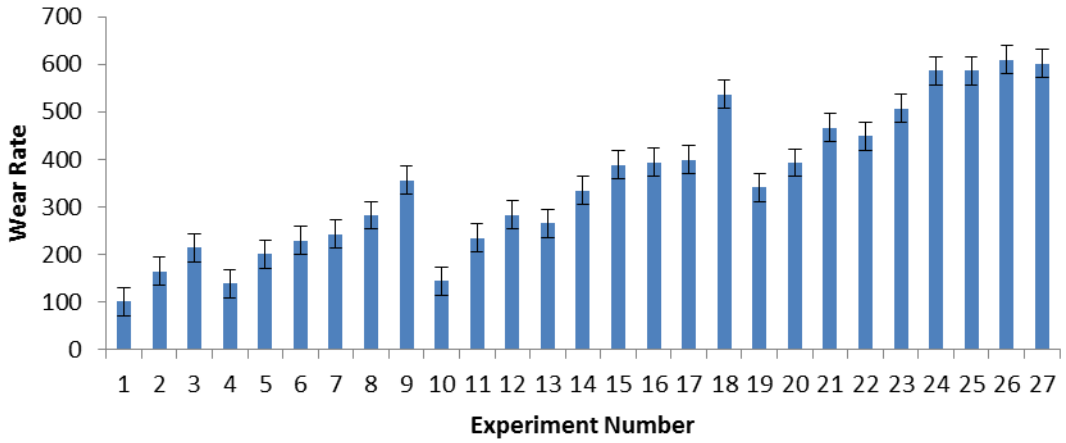

Figure 2: (a) Frictional Force (b) Wear Rate

3. Results and Discussions

3.1 Grey relational analysis (GRA)

The grey relational approach does provide an effective response to the complexity and multi-input form challenges. When determining production technical requirements, grey relational evaluation may consider machining efficiency with potential pressure. The GRA was chosen to try to optimize several characteristics at the same time.

*3.3.1 S/N ratio and Normalization***.** Equation 3 has been utilized to measure the S/N ratio:

Smaller the better: $$\frac{S}{N_{SB}} = -10\ \log_{10}\left[\frac{1}{n}\left(\sum_{i=1}^{n} y_{ij}^{2}\right)\right] \qquad (1)$$

Which y_{ij} is the i^{th} analysis on the j^{th} testing, n is the overall value of testing conducted.

The grey relation seems to be the process of connecting the data recorded on the 'n' series of studies to be set between 0 and 1 to normalize to eliminate the different number of products and to minimize the variance in the observation. More consistency could produce better results in general.

Smaller the best $x_{ij}=\frac{[max_j y_{ij} - X_{ij}]}{[max_j y_{iy} - min_j y_{ij}]}$ (2)

where y_{ij} is the i^{th} analysis in the j^{th} testing. Using Equation 4, the S/N ratio and standardization calculation are presented in Table 2.

Table 2. S/N ratio and the normalization

Ex no	S/N Ratio		Normalization	
	Wear Rate	Friction Force	Wear Rate	Friction Force
1.	40.08643	-16.6502	0	1
2.	44.3487	-20.172	0.12576	0.723577
3.	46.60828	-17.6163	0.222109	0.934959
4.	42.85219	-18.1697	0.074437	0.894309
5.	46.06392	-18.9878	0.196557	0.829268
6.	47.22546	-20.5877	0.253085	0.682927
7.	47.7194	-19.0849	0.279511	0.821138
8.	49.02492	-20.0864	0.357041	0.731707
9.	51.03126	-22.6708	0.501401	0.447154

10.	43.20292	-20.0864	0.085684	0.731707
11.	47.42273	-21.2892	0.263459	0.609756
12.	49.05049	-21.9382	0.358679	0.536585
13.	48.49521	-22.1442	0.324173	0.512195
14.	50.48456	-22.5421	0.458705	0.463415
15.	51.77663	-22.9226	0.564117	0.414634
16.	51.89358	-22.3454	0.574455	0.487805
17.	52.01946	-22.9844	0.585739	0.406504
18.	54.5857	-23.3463	0.855312	0.357724
19.	50.64612	-23.1067	0.471044	0.390244
20.	51.8899	-23.6369	0.574127	0.317073
21.	53.37772	-24.5577	0.718487	0.178862
22.	53.04457	-24.0824	0.683981	0.252033
23.	54.10745	-24.0279	0.798857	0.260163
24.	55.35603	-24.9595	0.953045	0.113821
25.	55.36262	-24.7609	0.953918	0.146341
26.	55.70317	-25.4368	1	0.03252
27.	55.57749	-25.6207	0.982783	0

3.3.2 Grey relation coefficient and grade.

Only at the actual levels of the experiment results does the grey coefficient relationship emphasize the significance of an enhanced objective feature of the experiment results.

$$\delta_{ij} = \frac{\min_i \min_j |X_i^0 - X_{ij}| + \zeta \max_i \max_j |X_i^0 - X_{ij}|}{|X_i^0 - X_{ij}| + \zeta \max_i \max_j |X_i^0 - X_{ij}|} \qquad (3)$$

there $x_i^0$to that j^{th} experiment becomes the appropriate normalized outcome,ζ becomes their coefficients which scale respectively 0 and 1. The assessment of the gray relationship will include the characteristics of the average grade relationship for each of the corresponding properties of output performance characteristics.

$$\gamma_j = \frac{1}{m}\sum \quad \zeta_{ij} \qquad (4)$$

there i=1 and m,$\gamma_j$inmth number of voltage attributes was the grey relationship classification of its j^{th} observation. Table 3 tabulates the grey relationship coefficient calculated through equation 5 but that GRD of the grade measured from formula 6. This method being assigned with (3-6).

Table 3. Grey relation grade and its order

Ex. No	Grey Relation Coefficient		GRG	Rank
	Wear Rate	Friction Force		
1	0.333333	1	0.666667	26
2	0.363837	0.643979	0.503908	11
3	0.39127	0.884892	0.638081	23
4	0.350739	0.825503	0.588121	20
5	0.383599	0.745455	0.564527	18
6	0.40099	0.61194	0.506465	12
7	0.409672	0.736527	0.573099	19
8	0.437461	0.650794	0.544127	16
9	0.500702	0.474903	0.487803	7

10	0.353528	0.650794	0.502161	10
11	0.404354	0.561644	0.482999	6
12	0.438089	0.518987	0.478538	3
13	0.425233	0.506173	0.465703	1
14	0.480171	0.482353	0.481262	4
15	0.534255	0.460674	0.497465	8
16	0.540222	0.493976	0.517099	15
17	0.54689	0.457249	0.502069	9
18	0.77557	0.437722	0.606646	21
19	0.48593	0.450549	0.46824	2
20	0.540031	0.42268	0.481356	5
21	0.639785	0.378462	0.509123	14
22	0.612731	0.400651	0.506691	13
23	0.713121	0.403279	0.5582	17
24	0.914152	0.360704	0.637428	22
25	0.915614	0.369369	0.642492	24
26	1	0.34072	0.67036	27
27	0.966712	0.333333	0.650023	25

3.3.3 Result analysis of grade relation grade.

The orthogonal network employs GRD to determine the optimal degree of settings. The higher the GRD, the better the efficiency of the computer. The best features of multiple responses lead to the second experimental state of an orthogonal network. The grey association class method is depicted in Table 4. The highest value of all levels of each is taken into account.

Table 4. Response table of the functional grey relation grade

Notations	**Machine factors**	**Response table**			**Maximum-Minimum**
		L 1	**L 2**	**L 3**	
A	Load(N)	0.5636	0.5038	**0.5693**	0.0656
B	Track Dia (mm)	0.5478	0.5321	**0.5568**	0.0248
C	Speed (rpm)	**0.5550**	0.5304	0.5514	0.0246
Error		0.5850	0.5539	0.5380	0.5448

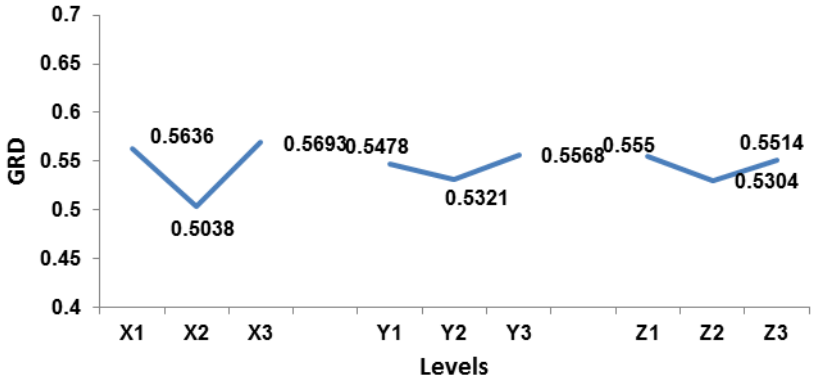

Figure 3. Grey relations grade vs Levels

Figure 3 depicts the ideal machining parameters at load at level 3, track diameter at level 3, and speed at level 1 based on each input parameter on GRD. The shift in observation indicates that each aspect is essential in determining exit responses.

3.3.4 Analysis of variance.

As per Table 5 of the ANOVA, the load has a major contribution as contrasted to the other entrance determining factors. Load has a 75.2 percent contribution, track diameter has a 17.2 percent contribution, and speed has a 3.6 percent contribution. The increase in load causes an increase in undue force on the surface, which results in an increase in friction force and an increase in friction coefficient. The wear speed improves at a load of 60 N and a track diameter of 60 mm, which could be due to the disc's nominal speed. As the speed of the disc increases, the working temperature causes the PLA materials to adhere to the surface of the sample. This further reduces the friction force discovered in experimental series number 26.A high friction rate is observed on experimental series of 27 at a high degree of disc speed.

Table 5. ANOVA results

Machine Factors	DOF	Sum of Square	Mean Square	% Contribution
Load(N)	2	0.0079	0.0040	76.8349
Track Dia	2	0.0009	0.0005	9.1386
Speed (rpm)	2	0.0011	0.0005	10.3093
Error	2	0.0004	0.00019	3.7172
Total	8	0.0103		100.0000

To verify the improvement in the characteristics of the optimal functioning condition (A3B3C1) using the predicted GRG Equation 9 was used:

$$\text{A3B3C1.}\hat{\Upsilon} = \gamma_m + \sum_{i=1}^{j}(\gamma_i - \gamma_m) \qquad (5)$$

Where$\hat{\Upsilon}$ is calculated GRG, γ_m is the sum of GRG mean, γi is the optimal level GRG mean and q is the number of the independent machine factors. Table 6 compares the expected and experimental results. There is a similarity with the A3B3C1. The test revealed that the expected and experimental system factors achieved by the GRG were 0.6545 and 0.6425, respectively. The enhancement of the GRG's output characteristics is attributed to the initial machining factors. Initial and predicted optimum inlet machining variables suggest a 0.0122 boost. The original and experimental optimum machining factors have improved by 0.0242. The experimental optimal machining variables, as predicted, had the fewest observations, demonstrating the performance improvement in the optimum working environment.

Table 6. Compliance with the confirmation experiment

Initial machine factors		**Optimal machining parameters**	
		Predicted	**Experimental**
Level	A1B1C1	A3B3C1	A3B3C1
GRG	0.6667	0.6545	0.6425
Improvement	---	0.0122	0.0242

4. Conclusion

Observations, it is known that the A3B3C1 (Load=40N; Track Dia=60mm & Speed=400 rpm) was found to be optimal for best exit responses, as confirmed by a confirmatory test. The higher working machine factors of load and track diameter at higher speeds provided an ideal environment for the fabricated composite. As compared to other machine variables, the test load plays an important role in deciding the machining parameters, accounting for 76.8 percent of the total. The influence of track diameter and speed is 9.1 percent and 10.3 percent, respectively.

References

1. Ahamad, S., Rat, P., Jedsada J. and Kittitat, S (2017) *Journal of Materials Chemistry C Vol. 5 , pp.4614-4620.*
2. Babu, T. V (2019) *Journal of Innovation in Mechanical Engineering Vol. 2, pp. 27-31*
3. Balamurugan, K., Uthayakumar, M., Sankarand, S., Warrier, K.G.K. (2018) *International Journal of Machining and Machinability of Materials Vol.19, pp.426–439.*
4. Evgeni, I., Rumiana, K., Hesheng, X., Yinghong, C., Ricardo, K. D., Katarzyna, D., Anna,D. M. Rosa, P. G., Sossio, C and Verislav, A (2019) *Applied Science. Vol. 9, pp. 120-1213*

5. Feng, Z., Min, W., Vilayanur, V.V., Benjamin, S., Yuyan, S., Gang W and Chi.,Z. (2017) *Nano Energy,Vol. 40, pp. 418–431.*
6. Gnanasekaran, K., Heijmans, T., Bennekom, S. V., Woldhuis, H., Wijnia, S. G. and Friedrich, H. (2017) *Applied Materials Today Vol. 9 (2017), pp. 21–28*
7. Jeyapaul, R. and Shahabudeen, P (2005) *International Journal of Advanced Manufacturing Technology, Vol.26, pp.1331-1337.*

8. Lebedev, S. M., Gefle, O. S., Amitov, E. T., Zhuravlev, D. V., Berchuk, D. Y and Mikutskiy, E. A (2018) *The International Journal of Advanced Manufacturing Technology 97 , pp.511–518*
9. Miguel, A.C., Ignacio, L.G., Nicolette, C. S., Jose, L. L. S., Teodolito, G. G., Juan, S. C .C. and Olga, S. B. (2018) *Additive Manufacturing Vol. 22, pp. 157–164.*
10. Najera, M. Sandra, J. Michel, K. Kyung and Namsoo (2018) *Journal of Material Science & Engineering. Vol. 07, pp. 10.*
11. Prakash, K. S., Gopal, P. M and Karthik, S. (2020) *Measurement. Vol. 157, pp.107664.*

12. Prashantha, K. and Roger, F. (2017) *Journal of Macromolecular Science, Part A Vol. 54, pp.24-29.*
13. Sheikh, M., Mahmud, T., Wolf, Ch., Glanz, C. and Kolaric, I (2010) *Composites Science and Technology, Elsevier , Vol. 70 (16), pp.2253-2259.*
14. Tuan, D.N., Alireza, K., Gabriele, I., Kate, T.Q.N. and H. David (2018) *Composites Part B Vol. 143, pp. 172–196.*
15. Uzair, K. Z., Emilien, B., Ali, S., Mickael, R and Aamer, A. B (2019) *The International Journal of Advanced Manufacturing Technology Vol. 101, pp.1215-1226*
16. Venkata Pavan, M and Balamurugan, K (2020) *Vol.10, pp. 843-852*.

17. Zhaobing, L., Qian, L. and Shuaiqi, X (2019) *Journal of materials research and academy Vol. 8, pp. 3741-3751*